Supporting Information

Tannous *et al.* 10.1073/pnas.0706802105

SI Text

Primary Culture of Neonatal Rat Ventricular Myocytes. Cardiomyocytes were isolated from the ventricles of 1- to 2-day-old Sprague–Dawley rat pups and plated as described (1) at a density of 1,250 cells/mm in medium containing 10% FCS with 100 μM BrdU. Myocyte cultures obtained using this differential plating method contained <10% noncardiomyocytes as determined microscopically by using a myocyte-specific α-actinin antibody (data not shown). Forty-eight hours postplating, cells were transferred to medium supplemented with 1% FBS, at which point treatment would begin.

Transient Transfection of Cultured Cardiomyocytes. Twenty-four hours after plating, NRVM were transfected with a GFP-tagged LC3 construct as described (2). Briefly, 0.5 μg of plasmid DNA was incubated for 15 min at room temperature with 50 μl Opti-MEM (Gibco 31985-070) and 3 μl of Plus reagent (Invitrogen 11514-015). This was then combined with preincubated Opti-MEM supplemented with 2 μl of Lipofectamine (Invitrogen 18324-012). Cells were washed twice with warm PBS, twice with prewarmed Opti-MEM, then incubated for 4 h with the DNA/Lipofectamine mixture. After this incubation period, cells were washed and treated as indicated.

Immunocytochemistry. Cultured cardiomyocytes were washed three times in PBS supplemented with calcium and magnesium. Cells were then fixed in 4% PFA, permeabilized for 2 min in 0.1% Triton-X 100, followed by 15-min blocking in PBS with 3% normal goat serum and 1% BSA. Primary and secondary antibody dilutions were identical to those used for our immunohistochemistry studies, described above. Immunostained sections were imaged by using a Zeiss LSM510 META laser scanning confocal microscope.

Adenoviral Infection of Cultured Cardiomyocytes. Experiments in which adenovirus expressing GFP (AdGFP)-infected cells were simultaneously labeled with a fluorescent-tagged antibody recognizing α-actinin demonstrated that adenoviral particles at a multiplicity of infection (MOI) of 50 or higher infected >90% of cells as described (3). For aggresome studies, NRVMs were infected 48 h postplating with adenovirus containing WT or mutant human CryAB (Ad-CryAB^{WT} and Ad-CryAB^{R120G}, respectively). Experiments were performed at MOI = 100, yielding a ≈95% infection rate. Cells were subsequently grown for 7 days in 2% FBS media supplemented with either rapamycin (10 nM) or 3MA (5 mM).

Cell Viability Measurements. NRVMs were cultured and infected as described above. Culture medium was changed every 24 h, and cell viability was measured after 5 days by the addition of 20 μl of CellTiter 96 AQ_{ueous} Solution Reagent (Promega G3580) to 100 μl of fresh culture medium. Cells were incubated for 2 h at 37°C in a humidified 5% CO_2 atmosphere, with absorbance then recorded at 490 nm by using a 96-well plate reader.

Subcellular Fractionation. NRVMs were harvested from 100-mm tissue culture plates in 100 μl of immunoprecipitation buffer (IPB) (10 mM Tris·HCl, 5 mM EDTA, 1% Nonidet P-40, 0.5% deoxycholate, 150 mM NaCl) and sheared by repeated passage through a 27-gauge needle. Lysates were incubated on ice for 30 min, and then centrifuged at 16,000 × *g* for 15min. The supernatant was collected and used as the soluble fraction. The insoluble pellet was resuspended in 10 mM Tris·HCl and 100 μl of 1% SDS and incubated at room temperature for 10 min. One hundred microliters of IPB was then added to the insoluble fraction, followed by 15 s of sonication.

Histology and Immunohistochemistry. Animals were euthanized with 5% sodium-pentobarbitol in PBS, pH 7.4 (n = 5, all groups). Hearts were fixed by sequential perfusion with 30 ml of heparinized PBS, 30 ml 4% paraformaldehyde (PFA), followed by overnight incubation in 4% PFA at 4°C with agitation before routine paraffin processing. All immunostaining was done on 5-μm sections cut in coronal orientation for four-chamber view. We performed antigen retrieval by microwave high-intensity epitope retrieval (HIER) using 1× Biogenex Citra (10 min at 95°C). When primary antibodies were of mouse origin sections were blocked and immunostained by using commercially available Mouse On Mouse immunodetection reagents (Vector BMK-2202). When not using mouse antibodies sections were blocked in 3% normal goat serum in PBS. Primary antibodies dilutions were: 1:30 CryAB (Vector VP-A103), 1:50 anti-MAP-LC3 (Santa Cruz sc-16756), 1:50 anti-vimentin (Santa Cruz sc-5565), 1:50 anti-ubiquitin (Santa Cruz sc-9133), 1:1,000 anti-ubiquitin (Abcam ab7254), or 1:50 γ-tubulin (Santa Cruz sc-10732). Routine hematoxylin and eosin, Masson's trichrome, and picrosirius red stains were performed according to established procedures (4, 5).

Electron Microscopy. Hearts were retrograde-perfused by using PBS and 2% glutaraldehydye in 0.1 M cacodylate buffer. Postfixation occurred in 2% osmium tetroxide in 0.1 M cacodylate buffer and 1% aqueous uranyl acetate each for 1 h. An ascending series of ethanol washes (50%, 70%, 90%, and 100%) was used to dehydrate the tissue followed by transitioning to propylene oxide and then a 1:1 mixture of propylene oxide and EMBED 812. The tissue was allowed to sit in EMBED for 1 h and then placed in a 70°C oven to polymerize the plastic. Sections were cut ≈75–80 nm in thickness by using a Leica ultramicrotome and a Diatome diamond knife, collected on 200-mesh copper grids, and poststained in 5% uranyl acetate in ethanol (for 10 min) and Reynold's lead citrate (for 5 min). A JEOL 1200 EX transmission electron microscope, operating at 40–120 V and equipped with a digital camera, was used to photograph the sections.

Immunoblot Analysis. Protein lysates were fractionated by SDS/PAGE, transferred to Hybond-C nitrocellulose membrane (HY-BOND-ECL Nitrocellulose), and subjected to immunoblot analysis. The ratio of antigen/antibody, detergent concentration, and duration and temperature of the reactions were optimized for each antibody.

Echocardiography. Transthoracic echocardiograms were recorded in conscious sedated mice as described (6). Left ventricular internal diameters and wall thicknesses were measured (at least three cardiac cycles) at end-systole and end-diastole from two-dimensionally targeted M-mode cross-sectional views at the level of the chordae tendineae. Heart rate was determined from mitral inflow Doppler envelopes.

Statistical Methods. Averaged data are reported as mean ± SEM. Statistical significance was analyzed by using Student's unpaired, two-tailed t test, or one-way ANOVA followed by Bonferroni's method for post hoc pairwise multiple comparisons. Comparison

of rates of aggregate accumulation was tested with logistic regression. The logit of the fraction of affected cells was modeled with main factors of cell line and time and a cell line × time interaction. The cell line difference between data points was estimated as a linear contrast within this model. Comparison of rates of decline in fractional shortening was tested with the log-rank statistic in a time-to-event context with events defined at the level of individual mice as attainment of 40% fractional shortening. SAS/STAT software, version 9.13, was used for all analyses.

1. Simpson P, McGrath A, Savion S (1982) Myocyte hypertrophy in neonatal rat heart cultures and its regulation by serum and by catecholamines. *Circ Res* 51:787–801.
2. Zhu H, *et al.* (2007) Cardiac autophagy is a maladaptive response to hemodynamic stress. *J Clin Invest* 117:1782–1793.
3. Richardson KE, *et al.* (2005) Guanosine triphosphatase activation occurs downstream of calcineurin in cardiac hypertrophy. *J Invest Med* 53:414–424.
4. Shehan DC, Hrapchak BB (1980) *Theory and Practice of Histotechnology* (C.V. Mosby Co., St. Louis, MO), 2nd Ed.
5. Woods AE, Ellis RC (1996) *Laboratory Histopathology: A Complete Reference* (Churchill-Livingston, New York).
6. Hill JA, *et al.* (2000) Cardiac hypertrophy is not a required compensatory response to short-term pressure overload. *Circulation* 101:2863–2869.

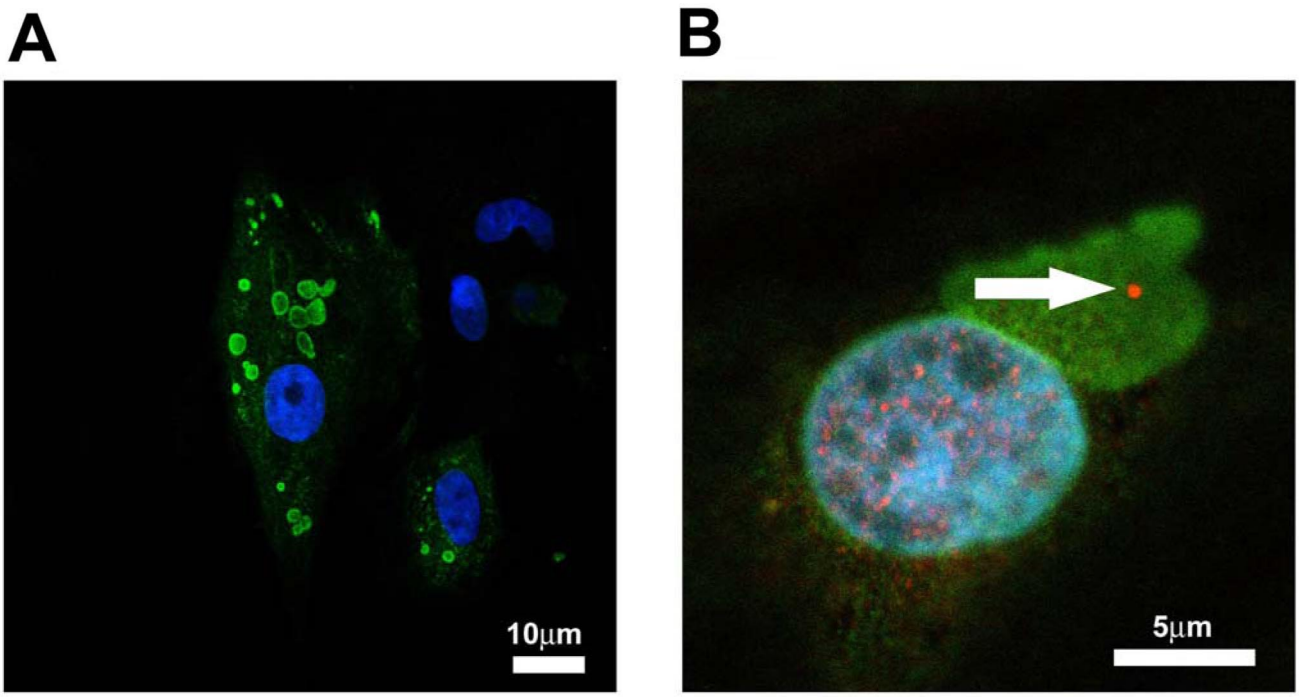

Fig. S1. Aggresome formation in DRCM. (*A*) Disruption of the microtubule network with nocodazole (10 μM) prevented coalescence of CryAB^{R120G}-associated aggregates at the microtubule organizing center (MTOC), consistent with aggresome formation. (*B*) Also consistent with aggresomes, coimmunostaining for CryAB and γ-tubulin (a component of the MTOC) demonstrated colocalization.

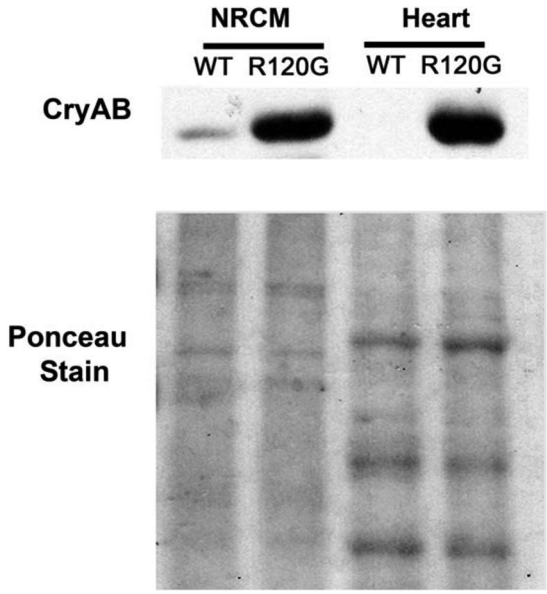

Fig. S2. Comparable levels of CryAB accumulation. Levels of transgenically expressed CryAB^{R120G} protein were comparable in the transgenic mice, relative to WT littermates, as compared with our *in vitro* overexpression studies in neonatal cardiomyocytes (NRCMs).

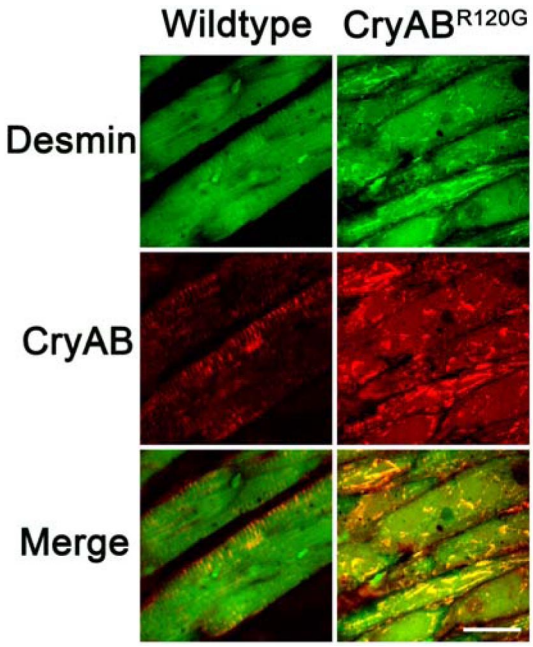

Fig. S3. Desmin colocalizes with CryAB. Coimmunostaining for desmin and CryAB demonstrated colocalization in *CryAB^{R120G}* hearts.

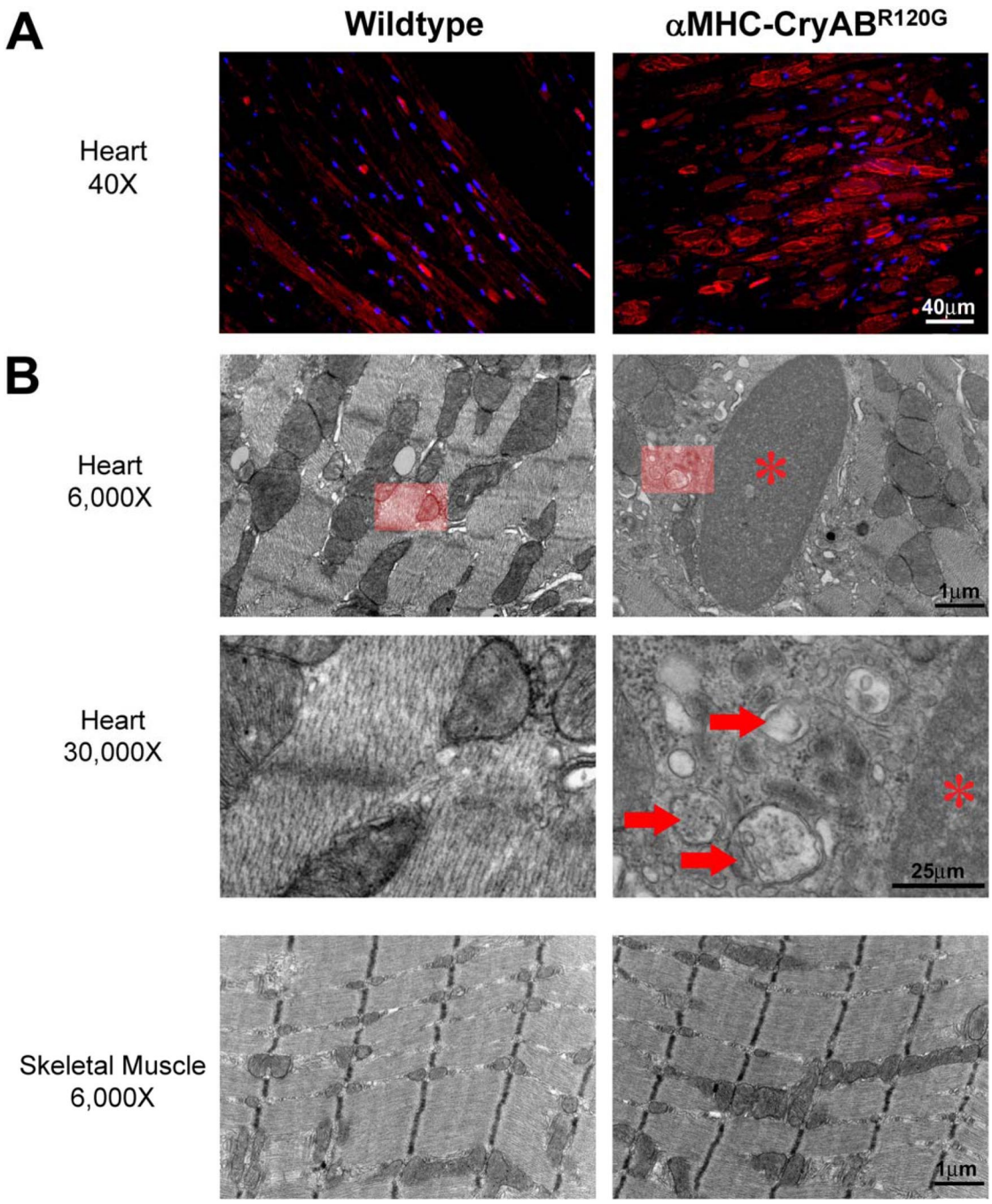

Fig. S4. Mutant CryAB expression induces autophagy *in vivo*. (*A*) Representative images (anti-CryAB immunohistochemistry) of a 2-month-old α*MHC-CryAB*^{R120G} mouse and a nontransgenic littermate. Extensive aggregate formation (asterisks) was detected in animals expressing mutant, but not WT, CryAB. (*B*) Ultrastructural analysis demonstrated morphological changes in the intersarcomeric region in α*MHC-CryAB*^{R120G} animals, including abundant accumulation of autophagosomes and myelin bodies (aged autophagosomes indicated by arrows). No such changes were observed in skeletal muscle from either genotype.

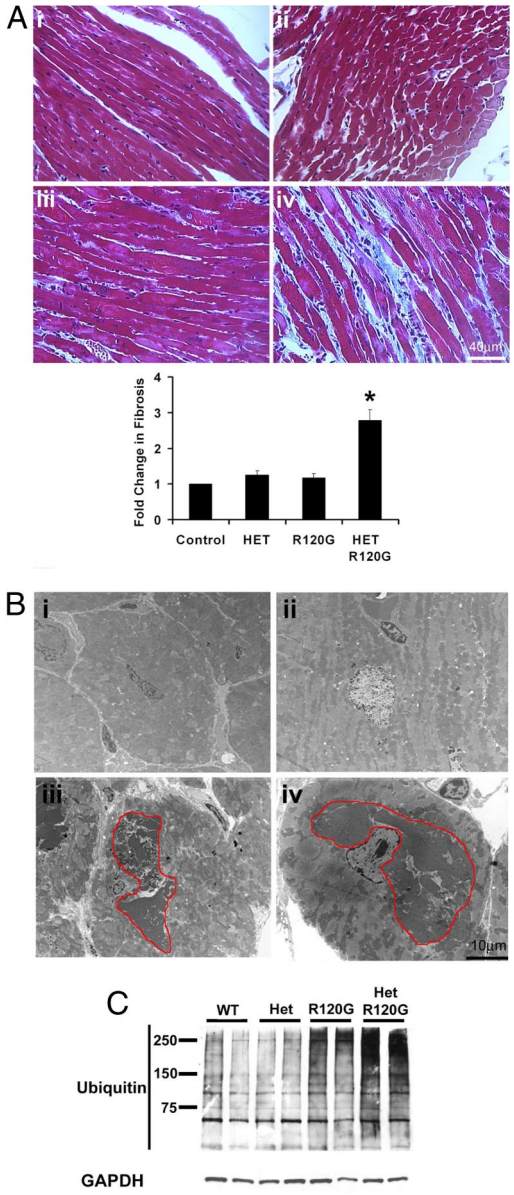

Fig. S5. Autophagy attenuates CryAB^{R120G}-induced pathological remodeling of the myocardium. (*A*) Representative paraffin-fixed sections from 9-month-old animals were stained with trichrome and imaged at ×40 magnification. Aggregate accumulation was detected in α*MHC-CryAB*^{R120G} animals, but consistent with the functional data, only minimal increases in total fibrosis were detected. Hearts from α*MHC-CryAB*^{R120G};*beclin 1*$^{+/-}$ mice, in contrast, contained extensive interstitial fibrosis, a sensitive marker of pathological cardiac remodeling. (*i*) WT. (*ii*) *beclin 1*$^{+/-}$. (*iii*) α*MHC-CryAB*^{R120G}. (*iv*) α*MHC-CryAB*^{R120G};*beclin 1*$^{+/-}$. (*B*) Transmission EM revealed similar patterns, where the blunting of autophagy triggered more extensive aggregate accumulation, with more severe pathological remodeling. (*C*) Representative immunoblots demonstrating extensive accumulation of high molecular mass ubiquitin-positive proteins in α*MHC-CryAB*^{R120G};*beclin 1*$^{+/-}$ mice relative to α*MHC-CryAB*^{R120G}, WT, or *beclin 1*$^{+/-}$.

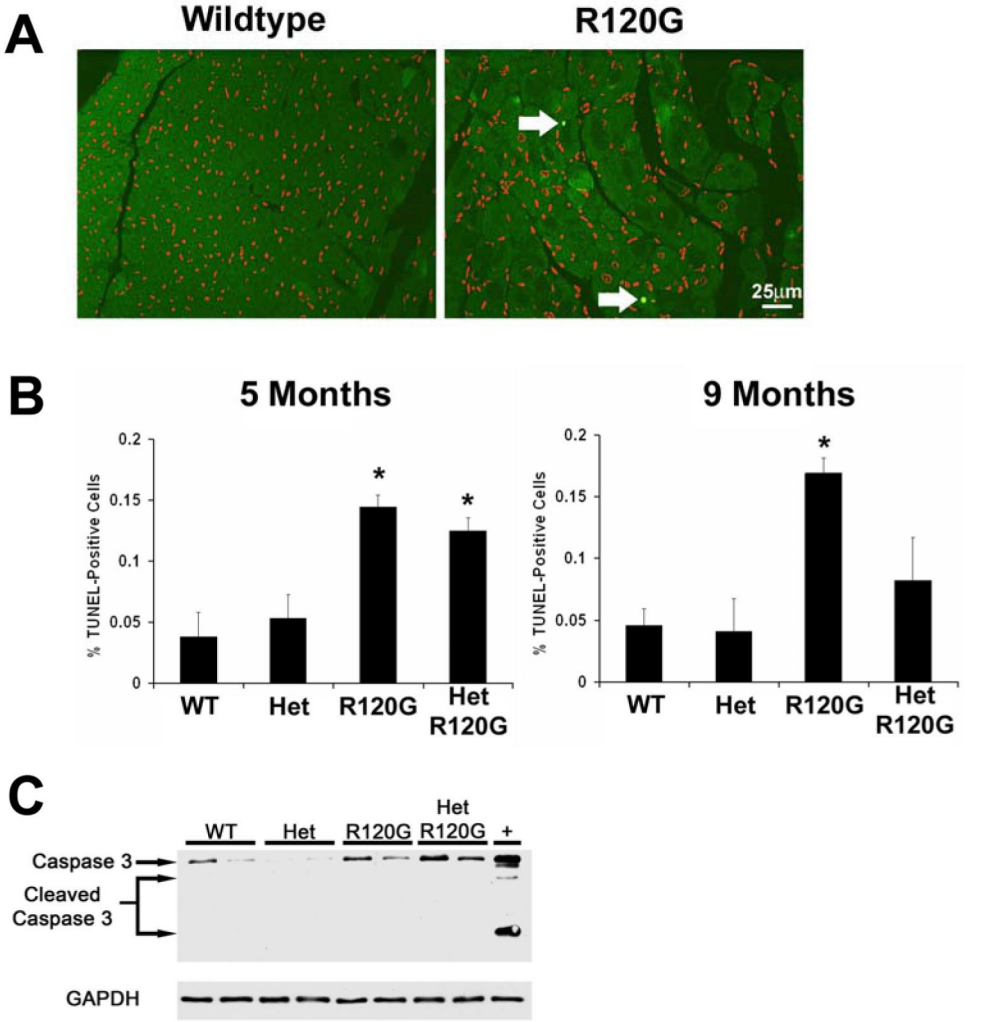

Fig. S6. Modest increases in apoptosis in DRCM. (*A*) Representative images of TUNEL staining performed in WT and *CryAB*^{R120G};*beclin 1*$^{+/-}$ hearts. These studies revealed only modest increases in cardiomyocyte apoptosis (arrows depict TUNEL-positive cells). (*B*) Apoptosis in 5- and 9-month-old animals was quantified as the proportion of TUNEL-positive cells with >7,000 cells counted per animal ($n = 3$ animals for each genotype). (*C*) Consistent with low level induction of apoptosis at 5 months of age, evidence of caspase 3 cleavage was not detectable by immunoblot analysis (+, positive control = staurosporine-treated NRVMs, 1 μM for 2 h).

Table S1. Echocardiographic data recorded at 9 months of age

Genotype	FS, %	LVIDd, cm	LVIDs, cm	Posteior wall, cm	HW/TL, mg/mm	LW/TL
WT ($n = 7$)	71 ± 0.9	0.225 ± 0.006	0.067 ± 0.003	0.153 ± 0.016	7.4 ± 0.9	9.5 ± 0.6
Beclin $1^{+/-}$ ($n = 9$)	69 ± 2	0.259 ± 0.012	0.085 ± 0.008	0.142 ± 0.001	7.6 ± 0.1	10.5 ± 0.2
R120G ($n = 8$)	59 ± 3*	0.228 ± 0.009	0.093 ± 0.006	0.193 ± 0.015*	10.7 ± 1.2*	10.5 ± 1.0
Beclin $1^{+/-}$ × R120G ($n = 8$)	39 ± 6‡	0.274 ± 0.04*	0.169 ± 0.041	0.183 ± 0.006*	10.9 ± 0.7*	9.8 ± 0.8

HW/TL, heart weight/tibia length; HW/LW, heart weight/lung weight.
*$P < 0.05$ relative to WT.
†$P < 0.05$ relative to R120G.